PHY180 Pendulum Project

Tianhao Fu
tianhao.fu@mail.utoronto.ca

Abstract

The experiment involving the behavior of a homemade pendulum yields results that disagree with the hypothesis of a constant period [4], but the symmetry and square root dependence of the period on length, as stated in the handout [4], hold, whereas the Q factor demonstrates a quadratic variance over length.

1. Introduction

The *PHY180 Pendulum Project* report studies the key characteristics of the kinematics of a real pendulum, specifically focusing on the dependence of the period, which is the time it takes to swing back to its starting position, on the initial angle and arm length individually, Q factor as a quality factor that measures the energy losses in the pendulum, as well as its dependence on length. Higher Q factors suggest higher energy losses, so that the pendulum will stop earlier.

The behavior of a pendulum is hypothesized to be a damped harmonic motion [4]:

$$\theta(t) = \theta_0 e^{-\frac{t}{\tau}} \cos(2\pi \frac{t}{T} + \phi_0) \tag{1}$$

where period T, in seconds, is predicted to be a constant [4]:

$$T \simeq 2\sqrt{r} \tag{2}$$

where r is the notation for the pendulum's equivalent arm length, in meters, in this report, since L is reserved for the string length. The Q factor is found by its definition [4]:

$$Q = \pi \frac{\tau}{T} \tag{3}$$

In the real pendulum, the period is concluded to be modeled by a quadratic function of initial angle:

$$T(\theta_0) = T_0(C\theta_0^2 + B\theta_0 + 1) \tag{4}$$

where $C = 0.040 \pm 0.001$, B is experimentally zero, and T_0, the predicted minimum period, is (1.441 ± 0.003)s. This relation rejects the hypothesis parameters that $B = C = 0$ [4]. It also implies a symmetry and an equivalently constant period for small initial angles. Using the *small angle approximation*, $\frac{\pi}{6}$ is chosen to be the initial angle for later experiments so that the period can be simplified as a constant with a 0.08% maximum error. The period-over-length data shows another feature of period as a square root function of arm length:

$$T(r) = kr^n \tag{5}$$

where $k = 2.00 \pm 0.01$ and $n = 0.491 \pm 0.008$, which fail to reject the hypothesis parameters that $k = 2, n = \frac{1}{2}$ [4].

The Q factor when the pendulum's arm length $r = 0.52$m is determined as the average of the values from the damped cosine fit, exponential fit, and number of oscillations to be:

$$Q(0.52\text{m}) = 78 \pm 2 \tag{6}$$

which is consistent with the quadratic relation with length found when the length varies:

$$Q(r) = c_1 r^2 + c_2 r + c_3 \tag{7}$$

where $c_1 = 70 \pm 40, c_2 = -150 \pm 50, c_3 = 140 \pm 10$. The Q factor is relatively low, meaning the energy efficiency of the pendulum is not ideal.

2. Methods and Procedures

2.1. Pendulum Setup

The pendulum consists of a string with some changeable length L, a 200g object, and a connector that hangs the mass onto the string. The string is passed through the connector and secured with two anchors that are 0.6m apart, as shown in Figure 1a. Note that the length of the rings at the two ends is not included in L. The triangular design restricts the motion of the object to only the plane that is perpendicular to the plane formed by the two string segments, also known as the oscillation plane. The connector is hot-glued to the center of the string, so that the object does not slide on the string, ensuring a constant radius. The equivalent arm length of this swing is derived in Section 5 as:

$$r = \frac{1}{2}\sqrt{L^2 - 0.36\text{m}^2} \tag{8}$$

Figure 1b demonstrates the initial appearance of the oscillation plane. θ_0 is the acute angle between the string and

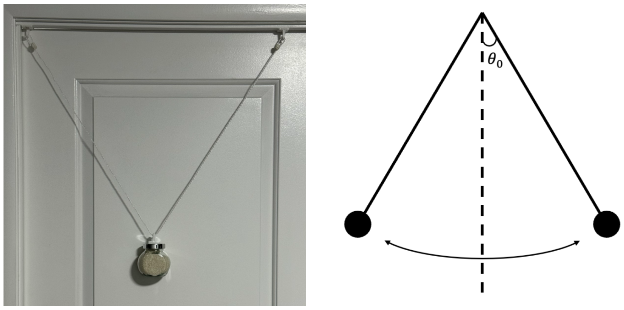

(a) The static view of the pendulum when $L = 1.2$m. The two anchors are attached to the door frame. The jar can swing back and forth when the door is open. The center joint is later hot-glued.

(b) Schematic diagram of the oscillation plane of the pendulum.

Figure 1. The front view and the side view of the pendulum.

the vertical axis from which the pendulum is released. A standard protractor measures the angle and ensures that the pendulum is released from the desired angle, and also introduces a Type B uncertainty:

$$u_b(\theta_0) = \frac{1}{2}^\circ = \frac{\pi}{360} \tag{9}$$

An iPhone 16 Pro is set to slow-motion mode at 240 frames per second in 1080p resolution and placed on a calibrated tripod such that the optical axis is orthogonal to the pendulum's oscillation plane. This results in a small Type B time uncertainty $u_b(t) = \frac{1}{2} \cdot \frac{1}{240}$s and a Type B angle uncertainty (see Section 5 for propagation). Since videos are analyzed in software, the Type A time uncertainty can be ignored:

$$u(t) = u_b(t) = \frac{1}{480}\text{s} \tag{10}$$

String A nylon string with a negligible mass smaller than 0.5g is chosen to minimize deformation, resulting in a negligible change in length.

Connector The connector is constructed by gluing a plastic hook onto the top of a plastic cap of a spice jar. The purpose of the connector is that the object can be attached to strings of different lengths.

Object A glass spice jar filled with rice is used as the object. A digital scale measures the total mass of the filled jar with cap to be 0.2kg.

2.2. Dependence of Period on Angle

The length of the string L is set to 1.2m, giving an equivalent radius $r = 0.52$m according to Equation 8.

For each $\theta_0 \in \{-90^\circ, -80^\circ, \ldots, 90^\circ\} \backslash \{0^\circ\}$, a video is recorded for one oscillation when the object returns near its initial position. The period T is given by $T(\theta_0) = \frac{i_f - i_i}{240}$ where i_i and i_f are the indices of the frames at which the object is released and swings back, respectively.

The procedure described above is repeated six times to reduce Type A uncertainty (see Section 5). Therefore, for each initial angle, there are six period values and a mean period.

2.3. Q Factor

The static setup follows the previous experiment in Section 2.2, thus the equivalent radius remains as $r = 0.52$m.

The object is released from $\theta_0 = 30^\circ$, which is validated by the *small angle approximation* (see Sections 3.1.3 and 5). A video is recorded until the object becomes roughly stationary. The *Tracker* [1] is used to measure the angle in every frame.

The procedure described above is repeated three times to not only reduce Type A uncertainty but also quantify the Type B uncertainty introduced by the tracker application. Three videos are aligned together so that they all start at the first frame where the angle changes. Therefore, in every frame, there are three angle values and a mean angle.

2.4. Dependence of Period and Q Factor on Length

Experiments described in Sections 2.2 and 2.3 are conducted repeatedly with $r \in \{0.3, 0.4, \ldots, 1.0\}$m since the projected view plane is roughly $0.8\text{m} \times 1.4\text{m}$ (see Section 5) with a 0.3m margin where perspective error becomes significant. Note that when finding the Q factors, instead of averaging all three methods, only the exponential fit is taken since it gives lower residuals with a higher R^2 value (see Section 3.2.4).

3. Results and Data Analysis

3.1. Dependence of Period on Angle

Using a best-fit parabola (see Section 5), the data suggest that period T is a function of angle θ_0:

$$T(\theta_0) = T_0(1 + B\theta_0 + C\theta_0^2) \tag{11}$$

with coefficients:

$$\begin{cases} T_0 = (1.441 \pm 0.003)\text{s} \\ B = 0.001 \pm 0.001 \\ C = 0.040 \pm 0.001 \end{cases}$$

3.1.1. Uncertainties

The Type A uncertainty of the period $u_a(T)$ is calculated using Equation 23. Therefore, the overall uncertainty of the period is defined as $u(T) = \max(u_a(T), u(t))$ because

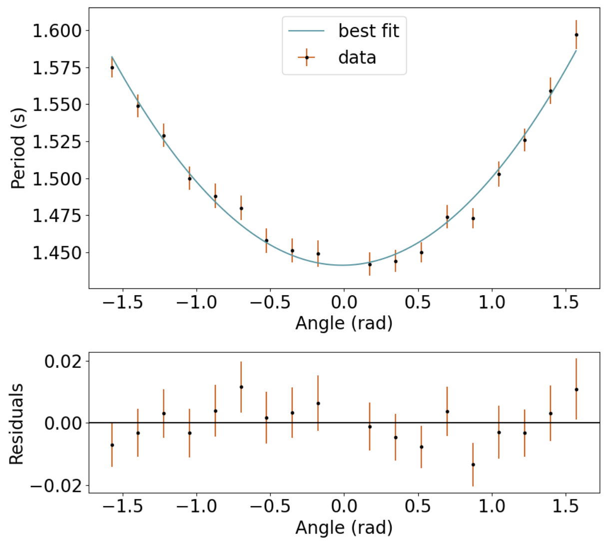

Figure 2. Period of the pendulum as a function of initial angle. Quadratic best-fit function 11 with parameters $T_0 = (1.441 \pm 0.003)$s, $B = 0.001 \pm 0.001$, $C = 0.040 \pm 0.001$ with $R^2 = 0.98$. Horizontal uncertainty 0.009 is too small to be seen (see Section 3.1.1).

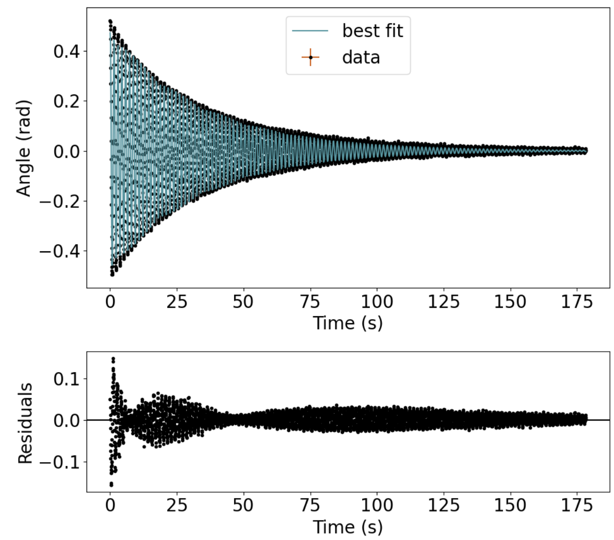

Figure 3. Angle over time. Damped-cosine best-fit function 12 with parameters $\theta_0 = 0.492 \pm 0.002, \tau_1 = (33.9 \pm 0.2)s, T = (1.44211 \pm 5 \times 10^{-5})s, \phi_0 = -0.281 \pm 0.004$ with $R^2 = 0.97$. All error bars (0.002s and 0.0007) are too small to be seen (see Section 3.2.3).

$u_b(T) = u(t)$. It is found in the collected data that $u(T) = u_a(T)$ and $u_{max}(T) = 0.01$s.

For the initial angle, there is no Type A uncertainty because the values are manually set. As a result, $u(\theta_0) = u_b(\theta_0) = 0.009$ based on Equation 9.

In the current setup, the major source of uncertainty is the variance in period. In the future, this can be optimized by adding more trials.

3.1.2. Residuals

Figure 2 includes a residual graph where the scatters distribute randomly around the zero. This represents a strong fit of the function, and there is no exceptional pattern; thus, a quadratic function is good enough.

3.1.3. Small Angle Approximation

From Figure 2, it can be approximated that when $\theta_0 \in [-\theta_{0s}, \theta_{0s}]$ where θ_{0s} is some small initial angle, $\frac{dT}{d\theta_0} \approx 0$. Therefore, the period can be roughly seen as a constant in the described small domain. This approximation is further verified in Section 5.

3.2. Q Factor

Tracker [1] analyzes 42792 frames and exports a data point (t, θ) for each frame, where θ has the same coordinate and convention system as θ_0 shown in Figure 1b.

The scatter plot (Figure 3) suggests a periodic relation between angle θ and time t:

$$\theta(t) = \theta_0 \mathrm{e}^{-\frac{t}{\tau_1}} \cos(2\pi \frac{t}{T} + \phi_0) \tag{12}$$

with coefficients:

$$\begin{cases} \theta_0 = 0.492 \pm 0.002 \\ \tau_1 = (33.9 \pm 0.2)\mathrm{s} \\ T = (1.44211 \pm 5 \times 10^{-5})\mathrm{s} \\ \phi_0 = -0.281 \pm 0.004 \end{cases}$$

$$Q_1 = \pi \frac{\tau_1}{T} = 73.9$$

3.2.1. Exponential Fit

Another method is used to acquire the Q factor. The local maxima points are selected using *SciPy* [3] to plot a decay trend in amplitude in Figure 4. The exponential best-fit curve is:

$$\theta_p(t) = A\mathrm{e}^{-\frac{t}{\tau_2}} \tag{13}$$

with coefficients:

$$\begin{cases} A = 0.482 \pm 0.003 \\ \tau_2 = (37.0 \pm 0.4)\mathrm{s} \end{cases}$$

$$Q_2 = \pi \frac{\tau_2}{T} = 80.6$$

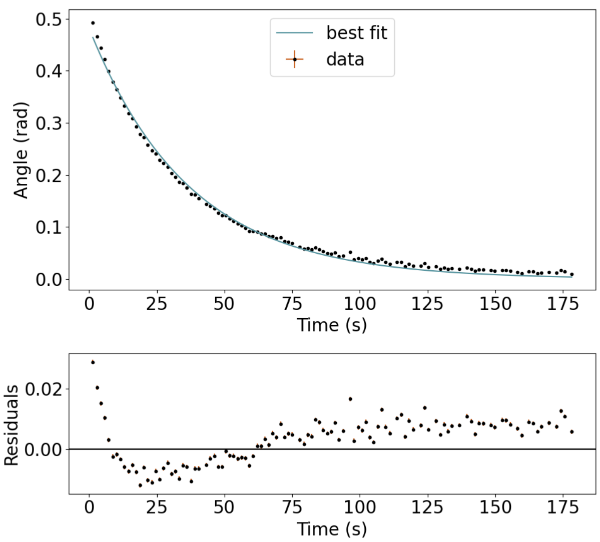

Figure 4. A plot of the upper peaks in angle as a function of time. Exponential best-fit function 13 with parameters $A = 0.482 \pm 0.003$, $\tau_2 = (37.0 \pm 0.4)$s with $R^2 = 1.00$. All error bars (0.002s and 0.0007) are too small to be seen (see Section 3.2.3).

3.2.2. Number of Oscillations

Another way to retrieve the Q factor is to count the number of oscillations it takes for the angle to reach 4% of the initial angle manually, which yields $Q_3 = 80.0 \pm 0.5$. The uncertainty is later derived in Section 3.2.3.

3.2.3. Uncertainties

Like the previous analysis in Section 3.1.1, the Type A uncertainty of the angle $u_a(\theta)$ is calculated using Equation 23. The Type B uncertainty is derived in Section 5 to be $u_b(\theta) = \frac{1\text{m}}{2700r} = 0.0007 > u_a(\theta)$, meaning that $u(\theta) = 0.0007$.

For the time axis, the overall uncertainty is determined in Equation 10 that $u(t) = 0.002$s.

Given the formula of the Q factor $Q = \pi\frac{\tau}{T}$, we can use the error propagation method to calculate the combined uncertainty $u(Q_1) = 0.4$ and $u(Q_2) = 0.9$ (see Section 5). The uncertainty of $Q_3 \in \mathbb{N}$ mainly comes from the low confidence in the determination of the frame index at which the pendulum is at the 4% amplitude threshold. It is previously established that $u(\theta) = 0.0007$. Near the end, $\Delta\theta \approx 0.008$ between two consecutive oscillations. Since $\Delta\theta > u(\theta)$, it is possible to determine that the target oscillation is either of two consecutive oscillations, so $u(Q_3) = \frac{1}{2}$.

$$\begin{cases} Q_1 = 73.9 \pm 0.4 \\ Q_2 = 80.6 \pm 0.9 \\ Q_3 = 80.0 \pm 0.5 \end{cases} \tag{14}$$

$$Q = \frac{Q_1 + Q_2 + Q_3}{3} \pm \max(\frac{\sigma}{\sqrt{3}}, u(Q_2)) = 78 \pm 2 \tag{15}$$

Note that the `find_peaks()` function in *SciPy*, which is used to find the local maxima points in Section 3.2.1, also introduces uncertainties. A minimum horizontal distance is asserted to be 1.4s. The function returns 109 data points as opposed to the expected number $\lceil\frac{180\text{s}}{1.44211\text{s}}\rceil = 125$.

The residuals imply that Figure 3 is noisier than Figure 4 because there are more data points, thus more distractions. Section 3.2.4 further examines in more detail. It explains the considerable difference between τ_1 and τ_2.

One way to reduce the largest primitive uncertainty $u_b(\theta)$ is to increase the video resolution.

3.2.4. Residuals

In Figure 3, there are greater residuals when $t \to 0$. The cause behind this tendency is that in the interval $[t_x, 180]$, as t_x increases, the variation of the graph decreases, meaning that deviating the parameters to the right data points satisfies more data points. For example, T is a function of the initial angle described by Equation 11. Each oscillation in Figure 3 can be seen as an independent trial, meaning that the period is a function such that $T(\theta)$, where θ is a function of time. Therefore, $T(\theta(t))$ is indirectly dependent on time. Near the beginning, the period is longer than the end. However, the change in the period is decreasing as time increases, meaning that a slightly smaller period satisfies more data points than a larger one. Therefore, the first few oscillations are weighted less, causing greater residuals.

The maximum-only view in Figure 4 also shares a similar pattern. The curvature of the exponential function is somewhat fixed. The parameters only control the rotational orientation. Since the right-hand side is flatter, leaning toward the right results in a lower residual sum than compromising to the left.

3.3. Dependence of Period on Length

The finite size of the bob is negligible. The offset of the center of mass of the bob is $R = 0.02$m away from the joint with the rope. Since $T \propto \sqrt{r}$ is predicted, $\frac{\Delta T}{T} \approx \frac{R}{2r} < 3\%$, where $r_{min} = 0.3$m. Refer to Section 5 for the derivation of the approximation.

The 8 data points observe a square root trend curve in Figure 5:

$$T(r) = k_1 r^{n_1} \tag{16}$$

with coefficients:

$$\begin{cases} k_1 = 1.997 \pm 0.007 \\ n_1 = 0.491 \pm 0.007 \end{cases}$$

Note that units for k and n are omitted as they are not quite meaningful when r is in meters and T is in seconds.

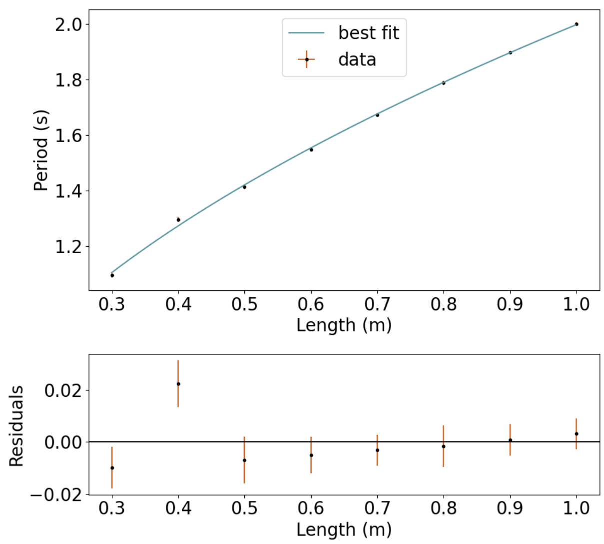

Figure 5. Period as a function of length 16 with parameters $k_1 = 1.997 \pm 0.007, n_1 = 0.491 \pm 0.007$ with $R^2 = 1.00$. Error bars for length (0.0004m) are too small to be seen (see Section 3.3.2).

3.3.1. Log-log Fit

$\ln x$ and $\ln y$, where (x, y) represents the same data points in the regular plot, are plotted in Figure 6:

$$T_{log}(r) = n_2 \ln r + \ln k_2 \tag{17}$$

with coefficients:

$$\begin{cases} \ln k_2 = 0.692 \pm 0.005, k_2 = 2.00 \pm 0.01 \\ n_2 = 0.491 \pm 0.008 \end{cases}$$

where k_2 and its uncertainty are later derived in Section 3.3.2.

3.3.2. Uncertainties

The uncertainties of the period are computed in the same way as in Section 3.1.1, and $u_{max}(T) = 0.01$s.

Since the desired arm length is manually set, there is no Type A uncertainty. The Type B uncertainty $u(r) = u_b(r) = 0.0004$m is computed with the formula derived in Section 5 evaluated at the L corresponding to $r = 0.3$m to get the maximum uncertainty.

The uncertainty for k_2 is given by exponential error propagation $u(k_2) = k_2 u(\ln k_2) = 0.01$, where $k_2 = e^{\ln k_2} = 2.00 \pm 0.01$. Therefore:

$$\begin{cases} k = \frac{k_1 + k_2}{2} = 2.00 \pm 0.01 \\ n = \frac{n_1 + n_2}{2} = 0.491 \pm 0.008 \end{cases} \tag{18}$$

Taking more trials can further minimize the largest intrinsic uncertainty, which is the Type A uncertainty of the period.

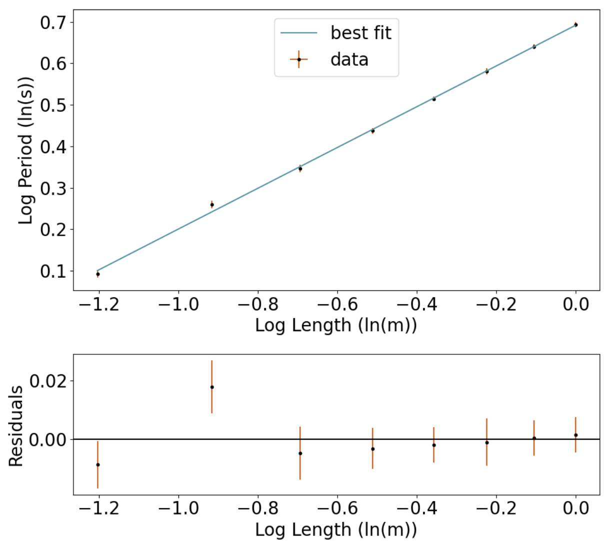

Figure 6. Log-log plot of period over length. Best-fit line 17 with parameters $n_2 = 0.491 \pm 0.008, \ln k_2 = 0.692 \pm 0.005$ with $R^2 = 1.00$. X error bars (0.0004m) are too small to be seen (see Section 3.3.2).

3.3.3. Residuals

The residuals in Figure 5 and Figure 6 are indications that the models fit well. They verify the confidence in the parameters together with the uncertainties.

3.4. Dependence of Q Factor on Length

Q factors acquired by exponential best-fit functions are plotted against length in Figure 7. The distribution shows a quadratic best-fit function:

$$Q(r) = c_1 r^2 + c_2 r + c_3 \tag{19}$$

with coefficients:

$$\begin{cases} c_1 = 70 \pm 40 \\ c_2 = -150 \pm 50 \\ c_3 = 140 \pm 10 \end{cases}$$

3.4.1. Uncertainties

Horizontal uncertainties $u(r) = 0.0004$m follow Section 3.3.2 and vertical uncertainties $u(Q) = 0.9$ follow Section 3.2.3.

The major source of natural uncertainty remains to be the Type A uncertainty of the period, which can be further optimized by taking more trials.

3.4.2. Residuals

The residual plot in Figure 7 indicates an outlier at $r = 0.4$m, explaining the high uncertainties. Other than that

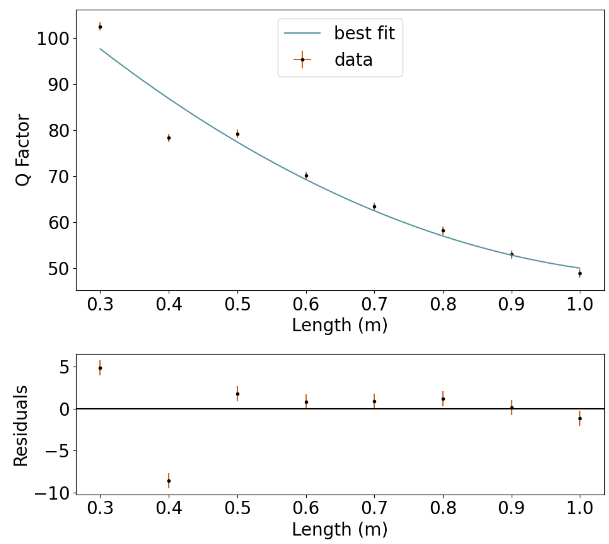

Figure 7. Q factor as a function of length 19 with parameters $c_1 = 70 \pm 40, c_2 = 150 \pm 50, c_3 = 140 \pm 10$ with $R^2 = 0.95$. X error bars (0.0004m) are too small to be seen (see Section 3.4.1).

outlier, the rest of the residuals distribute randomly around zero, which means the quadratic relation is able to capture most features.

4. Conclusion

4.1. Dependence of Period on Angle

Since the uncertainties are sufficiently low, there is a high confidence that the concluded model (Equation 11) **disagrees** with the hypothesis [4] that $C = 0$ because C is significant, given that $C > 3u(C)$. However, B is experimentally zero since $B = 0.000914 < u(B)$, which is consistent with the prediction and expected because of the symmetric nature of pendulums. Overall, it is shown that the period is dependent on the initial angle.

4.2. Q Factor

The Q factor $Q = 78 \pm 2$ measures energy lost in one oscillation:

$$E_f = E_i(1 - \frac{2\pi}{Q}) = 0.92 \tag{20}$$

which means the pendulum loses around 8% energy during each oscillation and implies a relatively high friction in the pendulum structure. As demonstrated in Figure 1a, the two anchors are made of rings hanging freely on hooks. The string rings can vibrate and slip on the hook, dissipating energy.

In the future, the two anchors can be hot-glued to reduce energy loss, increasing the Q factor.

4.3. Dependence of Period on Length

With all data points falling near the best-fit function within small uncertainties using both methods (direct fit and log-log fit), there is high confidence in the conclusion that the observation highly **agrees** with the hypothesized model $T = 2\sqrt{r}$.

This aligns with the formula $T = 2\pi\sqrt{\frac{r}{g}}$ as if we substitute in $g = 9.81\frac{\mathrm{m}}{\mathrm{s}^2}$:

$$T = \frac{3.14}{\sqrt{9.81}} \cdot 2\sqrt{r} = 1.003 \times 2\sqrt{r} \approx 2\sqrt{r} \tag{21}$$

4.4. Dependence of Q Factor on Length

To simplify the relation, the data point at $r = 0.4$m in Figure 7 is interpreted as an outlier and then it is observed to be a quadratic function:

$$Q(r) = (70 \pm 40)r^2 - (150 \pm 50)r + 140 \pm 10 \tag{22}$$

where the uncertainties are high because of the outlier.

The quadratic fit implies a local minimum near $r \approx 1.1$m, slightly beyond the largest radius that was measured. This prediction is uncertain because of the large uncertainties of the parameters, and it is not compared to simpler models. To test whether a real minimum exists, further experiments could be conducted with longer radii on either side of the predicted minimum, measure Q with higher precision at each length, and then compare constant, linear, and quadratic fits. Observing Q decreasing and then increasing again, with the turning point lying within the measured range and statistically significant compared to the error bars, would support the existence of a genuine local minimum.

PHY180 Pendulum Project

Supplementary Material

5. Appendix

5.1. Equivalent Radius of a Swing

Given a double-arm pendulum like the one in Figure 1a, the equivalent radius r is the perpendicular distance from the connector to the center of the two anchors, calculated by the Pythagorean theorem:

$$r = \frac{1}{2}\sqrt{L^2 - d^2} = \frac{1}{2}\sqrt{L^2 - 0.36\text{m}^2}$$

where $d = 0.6\text{m}$ is the distance between the two anchors listed in Section 2.1.

5.1.1. Center of Mass Approximation

Apply Taylor expansion onto $T(r) = 2\pi\sqrt{\frac{r}{g}}$:

$$\frac{\Delta T}{T} \approx \frac{\frac{\pi R}{\sqrt{rg}}}{2\pi\sqrt{\frac{r}{g}}} = \frac{R}{2r}$$

5.2. Trend of Type A Uncertainty

Type A uncertainty is given by:

$$u(X) = \frac{\sigma(X)}{\sqrt{|X|}} \tag{23}$$

where X is a set of samples, $\sigma(X)$ is the sample standard deviation of X, and $|X|$ is the number of samples. Assuming X follows some specific Gaussian distribution, $\sigma(X)$ is approximately independent from $|X|$. Therefore, when the number of samples increases, $u(x)$ is predicted to decrease.

5.3. Propagation of Type B Length Uncertainty

Given Equation 8, where $u_b(L) = \frac{1}{2}\text{mm} = 0.0005\text{m}$:

$$u_b(r) = |\frac{dr}{dL}|u_b(L) = \frac{0.0005L}{2\sqrt{L^2 - 0.36\text{m}^2}}$$

5.4. Propagation of Q Factor Uncertainty

Assume τ and T are uncorrelated. The uncertainty of Q is propagated by:

$$u(Q) = \sqrt{(\frac{\partial Q}{\partial \tau}u(\tau))^2 + (\frac{\partial Q}{\partial T}u(T))^2}$$
$$= \sqrt{(\frac{\pi}{T}u(\tau))^2 + (\frac{\pi\tau}{T^2}u(T))^2}$$

where the variables and uncertainties are given in Equations 12 and 13, thus:

$$\begin{cases} u(Q_1) = 0.4 \\ u(Q_2) = 0.9 \end{cases}$$

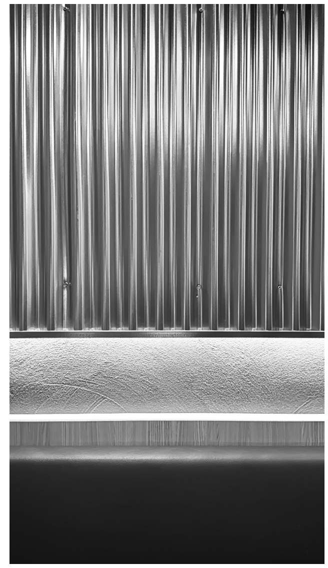

Figure 8. A frame taken with the identical configuration as used for recording videos. The optical axis of the camera is nearly orthogonal to the wall, so that the area of the projection plane can be estimated. About eleven and a half columns are in view.

5.5. Propagation of Type B Angle Uncertainty

In the selected video analysis software, the angle is calculated by:

$$\theta = \arctan(\frac{x}{y}) \tag{24}$$

Figure 8 is taken under the same settings as stated in Section 2.1. Given that each column is 7cm wide, the projection plane has a shape of approximately $0.8\text{m} \times 1.4\text{m}$.

Since the video has a definite resolution of 1080 by 1920, assuming square pixels, each pixel projects into $(\frac{0.8}{1080}\text{m})^2$. Therefore, the Type B uncertainty of position is:

$$u_b(x) = u_b(y) = \frac{1}{2} \cdot \frac{0.8}{1080}\text{m}$$

For function $\theta(x, y)$, assuming x and y are uncorrelated:

$$u_b(\theta) = \sqrt{(\frac{\partial\theta}{\partial x}u_b(x))^2 + (\frac{\partial\theta}{\partial y}u_b(y))^2} = \frac{u_b(x)}{\sqrt{x^2 + y^2}}$$

Since $\sqrt{x^2 + y^2} = r$:

$$u_b(\theta) = \frac{1\text{m}}{2700r}$$

5.6. Best-fit Function

Data are imported from a CSV file into *NumPy* arrays using *Pandas*.

Given a target function such as $f(x) = a+bx+cx^2+\ldots$, *SciPy* finds the coefficients $\{a, b, c, d\}$ that minimize the residuals using the Levenberg-Marquardt algorithm through least squares [2].

The uncertainties of the coefficients are retrieved in Equation 23 where the standard deviation σ is given by `curve_fit()` [2].

The R-squared value measures the coverage of the regression:

$$\begin{cases} SS_{res} = \sum_i (y_i - f(x_i))^2 \\ SS_{tot} = \sum_i (y_i - \bar{y})^2 \end{cases}$$

where R is the set of residuals and $y = f(x)$. The R^2 value is then:

$$R^2 = 1 - \frac{SS_{res}}{SS_{tot}}$$

5.7. Small Angle Approximation Validity

Continuing Section 3.1.3, when the pendulum is released from $30°$, the maximum change in period is:

$$\Delta T_{max} = \max(T(-\theta_{0s}), T(\theta_{0s})) - T_0$$

where T_0 is the minimum period derived in Equation 11. Since $T(\theta_0)$ is concave up, by definition $\max(T(-\theta_{0s}), T(\theta_{0s})) > T_0$. Substituting $\theta_{0s} = \frac{\pi}{6}$ in gives:

$$\Delta T_{max} = 1.44211\text{s} - 1.441\text{s} = 0.00111\text{s}$$

$$\frac{\Delta T_{max}}{T_0} = 0.08\%$$

which agrees with the guess in Section 3.1.3 that the change in period for $\theta_0 \in [-\frac{\pi}{6}, \frac{\pi}{6}]$ is negligible.

This is later agreed by the best-fit function Equation 12 where $T = (1.44211 \pm 5 \times 10^{-5})$s.

References

[1] Douglas Brown, Wolfgang Christian, and Robert M. Hanson. Tracker video analysis and modelling tool for physics education. https://opensourcephysics.github.io/tracker-website/, 2025. Accessed: 2025-09-30. 2, 3

[2] The SciPy Community. scipy.optimize.curve_fit — scipy v1.x manual. https://docs.scipy.org/doc/scipy/reference/generated/scipy.optimize.curve_fit.html, 2025. Accessed: 2025-09-30. 2

[3] The SciPy Community. scipy.signal.find_peaks — scipy v1.x manual. https://docs.scipy.org/doc/scipy/reference/generated/scipy.signal.find_peaks.html, 2025. Accessed: 2025-09-30. 3

[4] Brian Wilson. *PHY180 Lab Project (2025)*. University of Toronto, 2025. Downloaded from Quercus. 1, 6